Full Paper

Propellants, Explosives, Pyrotechnics

DOI: 10.1002/prep.201900092

Effect of Temperature on Shock Initiation of RDX-Based Aluminized Explosives

Pin Zhao,[a] Lang Chen,*[a] Kun Yang,[a] Deshen Geng,[a] Jianying Lu,[a] and Junying Wu[a]

Abstract: An increase in temperature of an explosive will lead shock sensitivity to change, which affects explosive safety. Therefore, a study of the effect of temperature on the shock initiation of explosives is of great significance. We carried out a series of tests on explosive-driven flyer-initiating heated RDX-based aluminized explosives (61 wt% RDX, 30 wt% Al, 9 wt% binder) and the temperature and input shock pressure of the explosives were controlled accurately during the tests. The pressure histories at different depths inside the explosives were measured by using manganin pressure gauges, and the effect of temperature on detonation wave growth was analysed. The ignition and growth reaction model, some parameters of which rely on temperature, was used to simulate the shock-initiation processes. The relationship between the model parameters and the temperature were obtained from the experimental results. The run distance to detonation as a function of the initial input pressure in a temperature range, the Pop plot, and the reaction degree of the explosives were determined. For the RDX-based aluminized explosives, binder softening and the increasing sensitivity of RDX are the two main reasons that change the shock sensitivity. For 25 °C–110 °C, the shock sensitivity decreases with an increase in temperature, mainly because of binder softening. However, for 110 °C–170 °C, the shock sensitivity increases with an increase in temperature, which depends on the increasing sensitivity of the RDX.

Keywords: Temperature · Shock initiation · Ignition and growth model · Reaction degree

1 Introduction

The shock sensitivity of explosives will change with an increase in temperature, which affects explosive safety. Therefore, a study of the influence of temperature on the shock sensitivity of explosives is of great importance. Schwartz [1] conducted shock-initiation experiments on heated TATB (1,3,5-Triamino-2,4,6-trinitrobenzene) -based mixed explosives by gas-gun driven projectile and found that the shock sensitivity increased with a higher explosive temperature. Since then, gas-gun-driven flyers impacting explosive charges for measuring pressure histories have been the main approach to study the effects of temperature on shock sensitivity. Urtiew et al. [2] carried out experiments on heated HMX (octahydro-1,3,5,7-tetranitro-1,3,5,7-tetrazocine)-based mixed explosives, by observing the pressure histories of explosive charges. They reported that the shock sensitivity of HMX will increase significantly when the crystal phase of HMX changes from β to δ at 190 °C. Vandersall et al. [3] performed impact-initiation tests on PBX9501 (95 wt% HMX, 2.5 wt% estane, 2.5 wt% plasticizer) at 150 °C, and the ignition and growth model parameters of the PBX9501 were calibrated at this temperature. Garcia et al. [4] applied initiation tests to RX-55-AA (95 wt% LLM-105, 5 wt% Viton) explosives at 25 °C and 150 °C and found that the volume expansion of LLM-105 that was caused by the increase of explosives temperature increased the shock sensitivity of the explosives. Gustavsen [5–7] completed shock-initiation experiments on PBX-9502 (95 wt% TATB, 5 wt% Kel-F800) by using a gas-gun driven non-magnetic stainless-steel flyer, by measuring the particle velocity inside the explosives at different temperatures and investigated the influence of temperature on shock sensitivity. Chen Lang et al. [8–9] proposed a test method for explosive-driven flyer-initiating explosives and achieved uniform explosive heating. Shock-initiation experiments were carried out on C-1 explosives (94 wt% CL-20, 6 wt% binder) at different heating temperatures, and the CL-20 crystal phase changed from ε to γ at 125 °C, which resulted in a weakening of the shock sensitivity. The function of the explosive parameters with temperature was given, and the shock sensitivity of the explosives at different temperatures was predicted. From the references, they provided an effective experimental method to study the shock sensitivity of explosive at different temperatures, which lays a foundation for studying shock sensitivity of explosive at different temperatures.

We performed shock-initiation experiments on RDX-based aluminized explosives by explosively driven flyers at

[a] *P. Zhao, L. Chen, K. Yang, D. Geng, J. Lu, J. Wu*
State Key Laboratory of Explosion and Science
Beijing Institute of Technology
No.5, Zhongguan South Street, Haidian District, Beijing, P.R. China
Fax: +86-10-6891 8035
**e-mail: chenlang@bit.edu.cn*

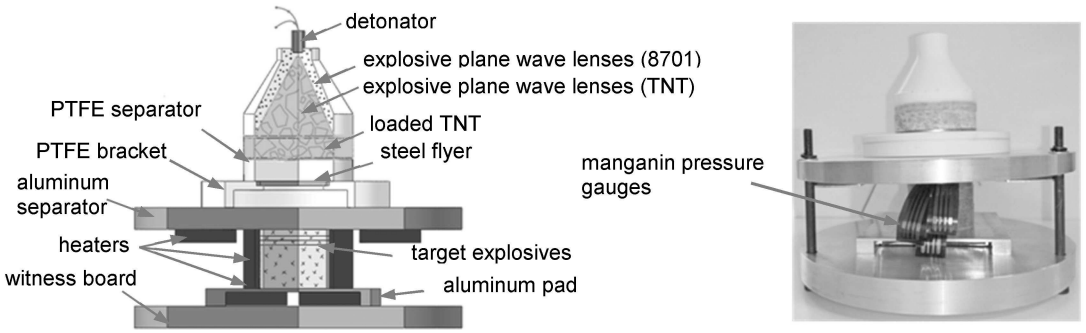

Figure 1. Profile (left) and photograph (right) of shock-initiation test device.

different temperatures. By measuring the wave-front pressure histories, variations in pressure were analysed. The shock-initiation model of the explosives was established by calculation, and the function of the reaction-rate parameters with temperature was studied. The reaction degree and the Pop plot of the explosives at various temperatures were calculated, and the effect of temperature on the shock sensitivity of the RDX-based aluminized explosives was investigated.

2 Shock-Initiation Tests on Heated Explosives

A test using an explosively driven flyer to initiate heated RDX-based aluminized explosive charges was designed. Figure 1 shows the profile and photograph of the test device, which consists of a detonator, explosive plane wave lenses, loaded TNT explosive, a PTFE(polytetrafluoroethylene) separator, a steel flyer, a PTFE bracket, an aluminum plate, an aluminum plate heater, an RDX-based aluminized explosive charges, manganin pressure gauges, thermocouples, an aluminum pad, an aluminum pad heater and other components. RDX-based aluminized explosives were pressed to 2- to 6-mm-thick explosive slices and 20-mm-thick explosive cylinders. At the center between the aluminum plate and the explosive slices, and between explosive slices, manganin pressure gauges were embedded to measure the pressure histories of the explosives, and a thermocouple was fixed at the center between the lower explosive slices and cylinders to monitor the internal explosive temperature. The heaters were electrified first, heat was transferred through the aluminum plate and the aluminum pad, and the temperature of the upper and lower surfaces of the explosives was controlled. When the temperature that was recorded by the thermocouple reached the preset temperature, it was considered that the tested explosives had been heated uniformly [9]. At this time, the detonator was electrified to initiate explosive lenses, and the lenses produced a planar shock wave, which was reduced by the PTFE separator to drive the flyer to impact charges. The heated RDX-based aluminized explosives were initiated by a shock wave, which was generated by the flyer impacting the aluminum separator. The pressure histories during the initiation processes were measured by the manganin pressure gauges at different depths from the impact surface of the explosives.

The explosive plane wave lens diameter was 50 mm and the loading explosive was TNT with a diameter of 50 mm and a height of 10 mm. The PTFE separator thicknesses were 6 mm, 10 mm and 14 mm. The aluminum plate thickness was 10 mm, the diameter of the steel flyer was 50 mm and its thickness was 3 mm. The diameter of the RDX-based aluminized explosives was 40 mm. The explosive charges were heated to the desired temperature by a rate of 5 K/min, then kept at this temperature for a while. When the center temperature of the explosive charges reached the desired temperature, the explosive charges were initiated. Shock initiation tests on the RDX-based aluminized explosives were carried out at 25 °C, 42 °C, 75 °C, 100 °C, 120 °C, 150 °C and 170 °C, respectively.

Figure 2 shows the measured pressure histories of the RDX-based aluminized explosives at different depths for the 10-mm PTFE separator at 25–150 °C. The growth characteristics of the detonation wave can be obtained from the pressure histories of the explosives. At 25 °C, the pressure increases to 4 GPa abruptly when the shock-wave front arrives at a 2-mm depth from the explosives impact surface. The pressure increases to 6 GPa after 0.25 μs and followed by a slow increase. These results indicate that the energy of the decomposition reaction does not support the shock-wave front propagation fully. When the shock wave reaches a 4 mm depth inside the explosive, the shock-wave-front pressure is 6 GPa, the pressure increases to 7 GPa smoothly after 0.1 μs, and then the pressure continues to increase slowly. These results suggest that the wave front pressure is enhanced. When the shock wave propagates to a 7-mm depth, the shock-wave-front pressure increases to 16 GPa, and after a slightly drop, it increases rapidly to 17 GPa, which indicates that the pressure is growing to detonation. These three pressure-versus-time curves can describe the growth characteristics of the detonation wave under shock initiation. At 75 °C, the pressure histories show that the ini-

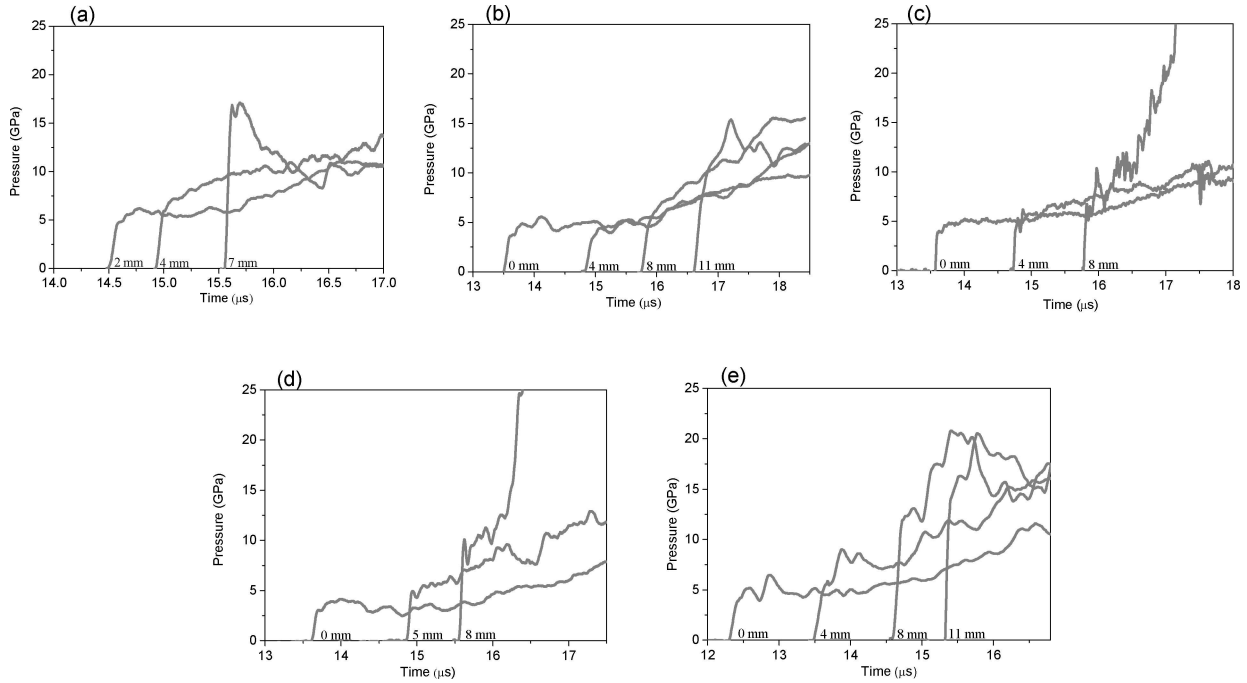

Figure 2. Measured pressure histories of RDX-based aluminized explosives at different depths under 10-mm PTFE separator at 25–150 °C. (a) 25 °C, (b) 75 °C, (c) 100 °C, (d) 120 °C, (e) 150 °C.

tial input shock-wave pressure is 4 GPa. However, when the shock wave reaches a 4-mm depth inside the explosives, the pressure decreases to only 3.5 GPa, which is 2.5 GPa lower than that at 25 °C. While the shock wave propagates to an 8-mm depth, the pressure just reaches 7 GPa, which is lower than the pressure of the 7-mm depth at 25 °C, and the shock-wave pressure increases to 15 GPa at a depth of 11 mm. Therefore, the run distance to detonation of explosives at 75 °C is longer than that at 25 °C, and we can conclude that the shock sensitivity of the explosives decreases with an increase in temperature. At 100 °C, the initial incident shock-wave pressure is 3.83 GPa, when the shock wave travels to a 4-mm depth inside the explosives, the shock-wave-front pressure is 5.22 GPa, and the pressure increases to 6.75 GPa at an 8-mm depth from the impact surface, which is lower than that at 75 °C. As the temperature continues to increase, the shock sensitivity of the explosives starts to decrease. At 120 °C, as shown in Figure 2 (b), at the explosives impact surface, the pressure is 3.5 GPa. While the shock wave front travels deeper in the explosives, the pressure increases to 5 GPa and 10 GPa, respectively, at a 5- and 8-mm depth from the initiation surface, which is higher than that at 100 °C, and shows that as the temperature increases, the shock sensitivity of the explosives is increased reversely. At 150 °C, the incident shock-wave pressure is 3.6 GPa. which is similar to the pressure at 120 °C. At a 4-mm depth from the impact surface of the explosive, the peak pressure of the shock wave is 9 GPa, and the peak pressure at 8 mm reaches 20 GPa, which is much higher than the same position at 120 °C. These results show that, as the temperature increases beyond 120 °C, the shock sensitivity of the explosives will be enhanced further.

The above test results show that the shock sensitivity of the RDX-based aluminized explosives decreases initially and then increases with an increase in temperature, which is different from the general law that the shock sensitivity of the explosives increases with an increase in temperature. We believe that binder softening and the increase in the shock sensitivity of RDX will influence the shock sensitivity. For 25–100 °C, binder softening has a greater influence on the shock sensitivity of the explosives. When the explosives temperature exceeds 120 °C, the increase in the shock sensitivity of RDX dominates.

3 Temperature-Considered Simulations of Shock Initiation on RDX-Based Aluminized Explosives

The pressure histories that were measured in the shock-initiation tests are limited, and it is difficult to investigate the complete shock-initiation law of the explosives, so a simulation of the shock initiation of RDX-based aluminized explosives is of great necessity. However, a method to exhibit the effects of temperature on the reaction rate is a key problem. We applied a three-term ignition and growth model [10] to describe the detonation reaction of the explosives. The influence of temperature on the reaction of

the explosives was investigated by establishing the relationship between the model parameters and the temperature, and the effects of temperature on the shock sensitivity for RDX-based aluminized explosives were analysed further.

A two-dimensional axisymmetric numerical simulation model was set up based on the shock-initiation explosive test device. The element size is 0.5 mm. The high explosive model and the products Jones-Wikins-Lee equation of state were used to describe the 8701 and TNT explosives in the explosive plane wave lenses, and the loaded explosive TNT. The PTFE separator, the aluminum separator and the steel flyer were calculated by using the elastoplastic hydrodynamic material model and the Grüneisen equation of state [9], and the ignition and growth-reaction rate model and JWL equation of state were applied to model RDX-based aluminum explosives.

The equations of the three-term ignition and growth reaction rate is [10]:

$$\frac{d\lambda}{dt} = I(1-\lambda)^b(\frac{\rho}{\rho_0}-1-a)^x + G_1(1-\lambda)^c\lambda^d P^y + G_2(1-\lambda)^e\lambda^g P^z \quad (1)$$

Where λ is the explosive reaction degree; t is the time; ρ is the density; ρ_0 is the initial density; P is the pressure and I, G_1, G_2, a, b, x, c, d, y, e, g, and z are constants. The first term on the right of the equation is the ignition term, the number of ignition hot spots are controlled by I and x, the latter two are the growth and completion term, the early growth of the hot spot after ignition is controlled by G_1 and d in the growth term. In the completion term, the reaction rate of explosives at a high pressure is determined by G_2 and z.

The unreacted and products JWL equations of state is [10]:

$$P_E = Ae^{-R_1V_E} + Be^{-R_1V_E} + \frac{\omega C_V T_0}{V_E} \quad (2)$$

$$P_p = Ae^{-R_2V_P} + Be^{-R_2V_P} + \frac{\omega C_V T_P}{V_P} \quad (3)$$

where P_E and P_p are the initial and products pressure, respectively; V_E and V_p are the initial relative volume and product relative volume of explosives, respectively; C_v is the heat capacity, T_0 and T_p are the initial temperature of the explosives and the product temperature, respectively; and A, B, R_1, R_2, and ω are constants.

RDX-based aluminized explosives consist of RDX, Al and binder, which are similar to the PBXN-109 explosive (64 wt% RDX, 20 wt% Al, 16 wt% binder). Therefore, the model parameters of the explosives were determined based on the ignition and growth model parameters and the JWL equations of state [11] of PBXN-109. The explosive parameters were calibrated at 25 °C by iterating over several possible values for the parameters and comparing and contrasting measured and calculated pressure histories at 25 °C.

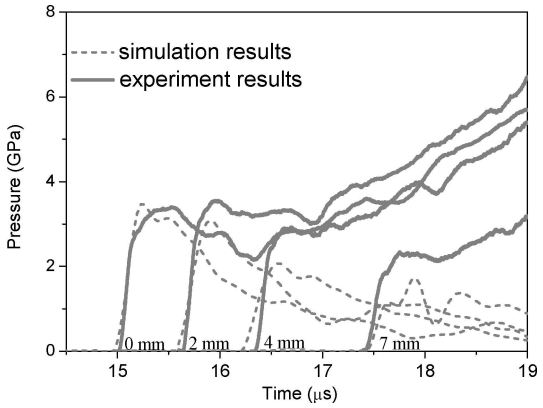

Figure 3. Measured and calculated pressure histories at different depths inside RDX-based aluminized explosives at 25 °C with 14-mm-thick PTFE separator.

In calculations, the wave-front pressure histories that were measured in tests were compared repeatedly with the input shock pressure of 2.3 GPa at the 14-mm thick PTFE separator, which didn't lead to a reaction, so that the parameters of the unreacted JWL equation of state were confirmed. Figure 3 shows the measured and calculated pressure histories of the shock-wave front at 25 °C with the 14-mm-thick PTFE separator. The initial-jump calculated pressure and overall decay trend are consistent with that in the tests, which suggests that the parameters that were applied in the calculations can describe the unreacted state of explosive basically.

The measured and calculated pressure histories and reaction degree for different impact strengths at 25 °C are shown in Figure 4. Figure 4(a) shows that the calculated initial jump pressure is consistent with the experimental pressure, and the overall variation trend of the pressure-time curves agrees closely with the experiment, which confirms that the model parameters that we used can characterize the shock initiation of the explosives. Additional simulations were run to verify the accuracy of the model parameters. Shock-initiation processes for the 6-mm-thick PTFE separator were simulated by using these parameters. As shown in Figure 4(b), the calculated pressure histories fit the experimental data well, which indicates that the calibrated model parameters can describe the initiation process basically. The model parameters are shown in Tables 1 and 2.

Figure 4(c) and 4(d) show the calculated reaction degree of the explosives for the 10- and 6-mm-thick PTFE separator, respectively. As the shock wave propagates deeper into the explosives, the reaction degree is increased gradually. The reaction rate at the same depth is faster with a higher impact strength. In Figure 4(c), when the shock wave arrived at a 2-mm depth inside the explosives, explosive decomposition starts to occur after 0.1 μs. From correspond-

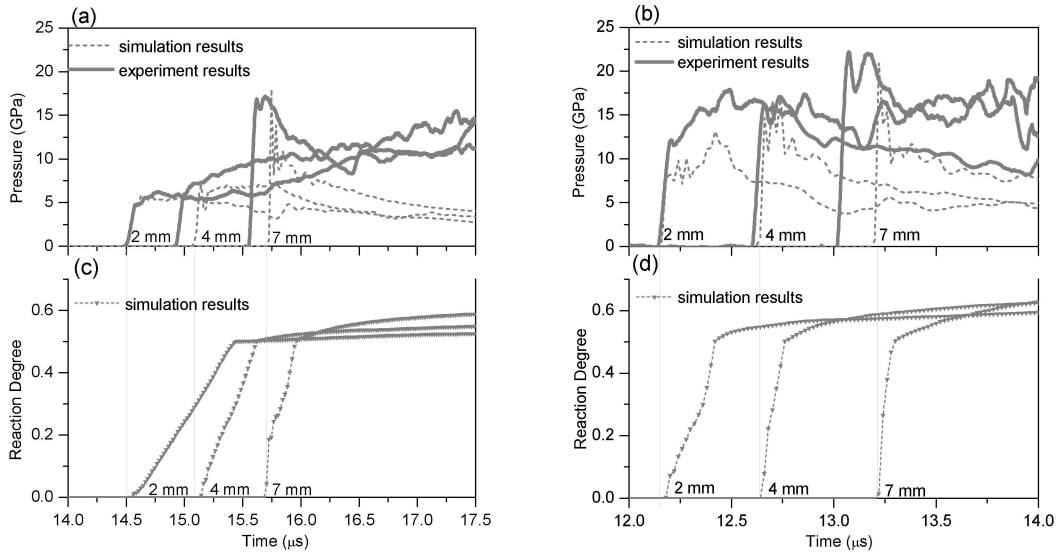

Figure 4. Measured and calculated pressure histories for different impact strengths at 25 °C, and calculated reaction degree-time curves of explosives. (a) and (c) 10-mm-thick PTFE separator, (b) and (d) 6-mm-thick PTFE separator.

Table 1. Parameters of JWL equation of state of unreacted explosive detonation products.

EOS	A(Mbar)	B(Mbar)	R_1	R_2	ω	C_V (10^{-5}Mbar·K^{-1})	E_0(Mbar)
UNREACTED JWL	8817	−0.0338	15	1.41	1.0	1.94	–
PRODUCTS JWL	13.413	0.327	6.0	2.0	2.0	1.0	0.102

Table 2. Parameters of reaction-rate equation.

I(μs^{-1})	a	b	c	d	e	g	x
4.55E + 04	0.02	0.667	0.667	0.667	0.3	1.0	8
y	z	F_{igmax}	F_{G1max}	F_{G2min}	G_1(Mbar^{-y} μs^{-1})	G_2(Mbar^{-y} μs^{-1})	–
2.0	3.0	0.22	0.5	0.3	450	550	–

ing pressure histories in Figure 4(a), it is obvious that the energy released by the explosives released by the explosives could not support wave-front propagation. As the wave travelled to a 4-mm depth, the explosives began to react on the front of the shock wave. However, the detonation wave was sustained by a small part of the energy only, which was provided by the explosives. When the shock wave reached a depth of 7 mm, a 0.52 reaction degree that assisted the detonation-wave growth was achieved on the shock wave front. At the high-intensity impact in Figure 4(d), and at a 2-mm depth from the impact surface, the detonation wave was supported by a small amount of energy, and at 4 mm and 7 mm, 0.50 reaction degree was reached, respectively, on the shock-wave front to sustain the detonation wave.

For the RDX-based aluminized explosives, binder softening, the increase in shock sensitivity of RDX, and volume expansion of the explosives are caused by an increase in temperature, which will lead to changes in the shock sensitivity. In the numerical simulations, the effect of temperature on the unreacted state of the explosives was highlighted mainly by adjusting parameter *B* in the unreacted JWL equation of state. By regulating G_1 in the ignition and growth models, the comprehensive effects of binder softening and the increased in shock sensitivity of RDX for higher temperatures on the shock sensitivity are described.

Through a volume-weighted average of the volume expansion coefficients of the components, the volume expansion coefficient of the RDX-based aluminized explosives at 25 °C was calculated. The explosive density at a higher temperature was determined according to the density and volume expansion coefficient of explosives at 25 °C.

The volume expansion coefficient of the explosives is:

$$\beta_v = \sum_{i=1}^{n} \alpha_i \beta_i \tag{4}$$

Table 3. Reaction-rate parameters of RDX-based aluminized explosives at different temperatures.

T_0(°C)	25	42	75	100	120	150	170
Density(g/cm^3)	1.770	1.763	1.739	1.730	1.723	1.713	1.706
B(Mbar)	−0.0327	−0.0351	−0.0376	−0.0395	−0.0410	−0.0433	−0.0448
G_1(Mbar^{-2} μs^{-1})	450	430	350	310	300	340	380

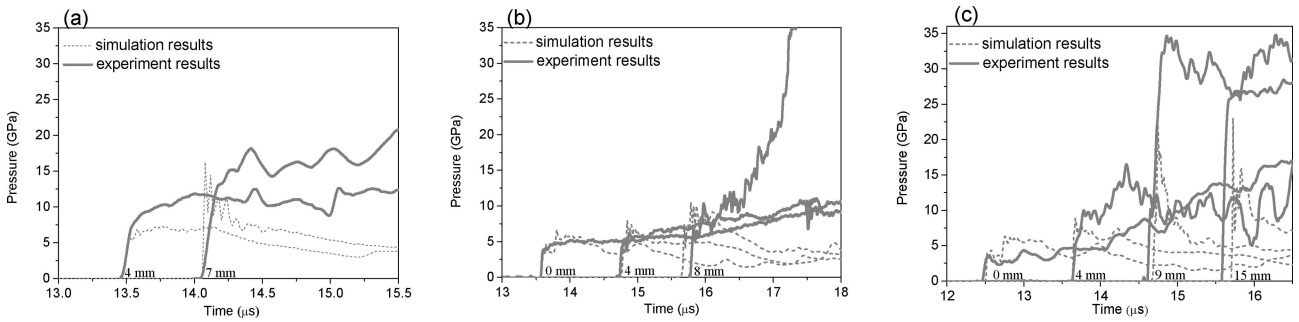

Figure 5. Calculated and measured pressure histories of different temperatures at different depths with 10-mm thick PTFE separator. (a) 42 °C, (b) 100 °C, (c) 170 °C.

where α is the volume fraction of each component, β_i is the volume expansion coefficient of each component, and β_v is the volume expansion coefficient of the mixed explosives ($^\circ C^{-1}$).

The density of the RDX-based aluminized explosives at different temperatures is calculated according to [6]:

$$\rho(T) = \frac{\rho(25\,^\circ C)}{(1 + (T - 25\,^\circ C)\beta_v)} \tag{5}$$

The volume expansion coefficient of RDX for 0–17 °C is $18.33\times10^{-5}\,^\circ C^{-1}$ [12], and the volume expansion coefficient of Al is $68.1\times10^{-6}\,^\circ C^{-1}$ [13]. Paraffin melts at 53.3–67.8 °C, the volume increases by 11% to 15%, the volume expansion coefficient of the solid phase is $10.1\times10^{-4}\,^\circ C^{-1}$, and the volume expansion coefficient of the liquid phase is $7.12\times10^{-4}\,^\circ C^{-1}$ [14].

B can be calculated at different temperatures at a standard atmospheric pressure by using Eq. (2). Numerical simulations were performed by using the obtained density and *B* at different temperatures, and parameters except G_1 in Table 2. in the ignition growth model at 25 °C and the JWL equations of state. The calculated pressure histories at different temperatures were compared repeatedly with the experimental pressure, and values of the growth term coefficient G_1 at different temperatures were obtained. Table 3. shows the density, *B* and G_1 of RDX-based aluminized explosives at different temperatures.

Figure 5 shows the calculated and measured pressure histories with different depths of explosives at 42 °C, 100 °C and 170 °C. The calculations agree well with the experiments at the initial jump time and pressure, and the tendency of the curves after the jump, which indicates that the model parameters and considered temperature variation can describe the effects of temperature on the shock initiation of RDX-based aluminized explosives.

Figure 6 shows the calculated reaction degree at a 4-mm depth from the impact surface of the RDX-based aluminized explosives at different temperatures, and Figure 6(a) shows the reaction degree curve at 42 °C, 75 °C and 100 °C. The reaction degree of the explosives increases rapidly to 0.5 in 0.3%s at 42 °C, and then increases slowly to 0.57 after 2.8%s. At 75 °C, the reaction degree of the explosives increased to 0.5 after 0.7%s, and then increased slowly to 0.53 in 2.3%s. However, when the initial explosives temperature was 100 °C, the reaction degree increased to only 0.47 within 3.5%s. It can also be concluded from Figure 7(a) that the shock sensitivity of the RDX-based aluminized explosives decreases with an increasing temperature below 100 °C.

Figure 6(b) shows the reaction degree curves of explosives at 120 °C, 150 °C and 170 °C. At 120 °C, the reaction degree increases slowly to 0.47 in 4.3%s, whereas at 150 °C, the reaction degree increases to 0.5 only in 1.4%s. When the temperature of the explosive was initialized to 170 °C, the reaction degree reached 0.5 in 0.8%s. These results reveal that when the temperature of the RDX-based aluminized explosives exceeds 120 °C, the shock sensitivity is enhanced with an increase in temperature.

Throughout the impact-initiation tests on the explosives, the shock-initiation law could be obtained at finite temperatures, so only the parameters of the reaction-rate model at tested temperatures can be determined. To achieve shock-initiation simulations on explosives at other temperatures, it is necessary to establish a function of the model parameters and temperatures, mainly to build up a

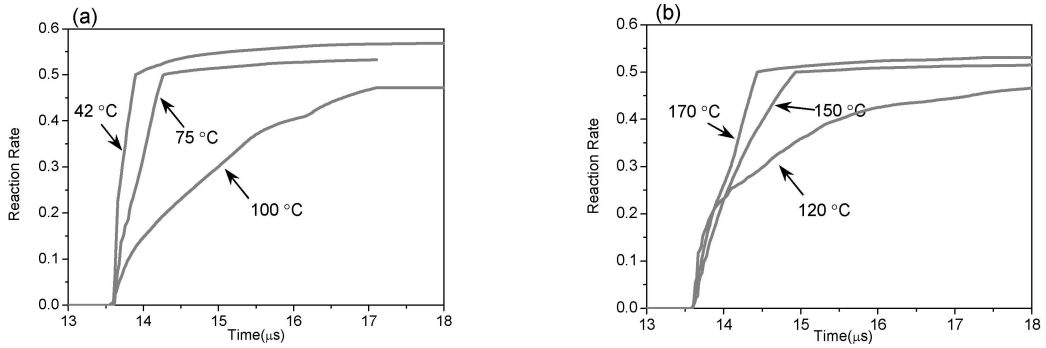

Figure 6. Reaction degree of explosives with different temperatures at 4-mm depth from impact surface. (a) Below 100 °C, (b) Exceeding 120 °C.

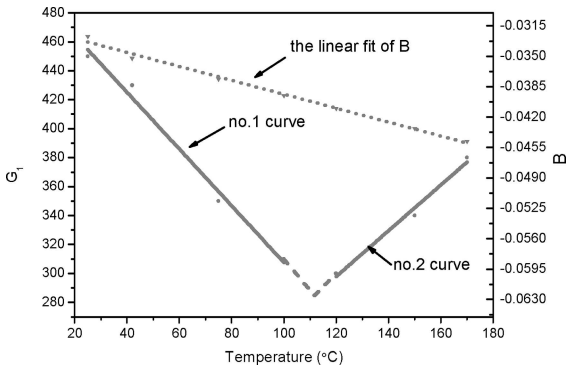

Figure 7. Relationship between G_1, B and temperature.

functional relationship between G_1 and temperature T [9]. Because the shock sensitivity of RDX-based aluminized explosives varies quite significantly with a variation in temperature, it is necessary to set up a functional relationship between G_1 and T in different temperature ranges. Based on the data in Table 3, two curves are obtained by piecewise fitting G_1 with the corresponding temperatures in ranges below 100 °C and above 120 °C, and dashed line is linear fit of B with temperatures, as shown in Figure 7. The variation of B values with different temperatures is roughly linear. No. 1 curve shows a linear decrease of G_1 for a temperature increase below 100 °C, whereas curve 2 shows a linear increase of G_1 with an increase in temperature above 120 °C. In the range of 100–120 °C the two straight lines are extended until they intersect, whereas the temperature at the intersection point is 111 °C, which can be regarded as the inflection point of G_1 with temperature, and the corresponding G_1 value is 284. Below 111 °C, the shock sensitivity of the RDX-based aluminized explosives decreases with an increase in temperature, and above 111 °C, the shock sensitivity of the explosives increases with an increase in temperature. At 111 °C, the shock sensitivity of the RDX-based aluminized explosives is lowest.

In the range of 25–170 °C, the fitting function of G_1 and the temperature is as follows:

$$G_1 = \begin{cases} 453 - 1.960(T - 25) & 25\,^{\circ}C \le T \le 111\,^{\circ}C \\ 284 + 1.579(T - 111) & 111\,^{\circ}C < T \le 170\,^{\circ}C \end{cases} \quad (6)$$

According to the functional relation of G_1 with T, the initiation of explosives at different temperatures and impact strengths can be modeled, and the relationship between the input shock-wave pressure and the run distance to detonation, Pop plot, can be obtained [15]. The quantitative variation law of the shock sensitivity with temperature was obtained. A model of the steel flyer impact RDX-based aluminized explosives was designed. By changing the velocity of the flyer impact to explosives, the incident shock-wave pressure was controlled. The run distance to detonation could be measured by calculating the pressure histories of the explosives. In the model, the flyer diameter was 50 mm with a thickness of 3.5 mm. The aluminum separator had a diameter of 50 mm and a thickness of 5 mm. The diameter of the explosives was 50 mm with a thickness of 30 mm. Many initiation calculations were carried out on the explosives at 25 °C, 60 °C, 111 °C and 160 °C. The Pop plot of the RDX-based aluminized explosives at 25 °C, 60 °C, 111 °C, and 160 °C was determined, as shown in Figure 8. The scat-

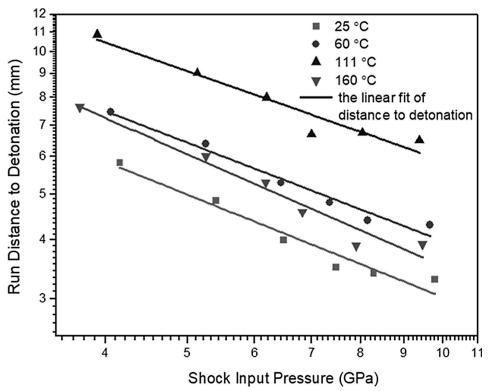

Figure 8. Pop-plot for RDX-based aluminized explosives at various temperatures.

ter is the run distance to detonation under different input pressure at different temperatures in simulation, and straight lines are linear fit of the run distance to detonation at different temperatures. From the trend of the Pop plot of explosives at different temperatures, we can establish that the shock sensitivity of the explosives is highest at 25 °C for the same incident shock pressure. The shock sensitivity of the explosives is lowest at 111 °C, and the shock sensitivity of the explosives at 160 °C was higher than that at 60 °C.

4 Conclusion

We performed tests of explosively driven flyer-initiating heated explosives and measured the pressure histories of RDX-based aluminized explosives at different heated temperatures. The function relationship of the ignition and growth model parameters G_1 with temperature was given, the reaction degree and Pop plot at different temperatures were modelled, and the effect of temperature on the shock sensitivity of RDX-based aluminized explosives was obtained.

An increase of temperature will result in binder softening and an increase in shock sensitivity of RDX, which will affect the shock sensitivity of the explosives. For 25 °C–111 °C, the explosives are affected mainly by binder softening, and the shock sensitivity decreases with an increase in temperature. When the temperature exceeds 111 °C, the influence of the binder is weakened, and the shock sensitivity is affected mainly by the shock sensitivity of RDX. These effects are strengthened as the temperature increases.

Acknowledgements

This work is supported by National Natural Science Foundation of China (NNSFC) under grant no.11832006.

References

[1] A. C. Schwartz, *Flyer Plate Performance and Initiation of Insensitive Explosives by Flyer Plate Impact*, Sandia Laboratory Report UCRL-50422, SAND, Albuquerque, NM, USA, **1975**.

[2] P. A. Urtiew, J. W. Forbes, C. M. Tarver, K. S. Vandersall, F. Garcia, D. W. Greenwood, P. C. Hsu, J. L. Maienschein, Shock Sensitivity of LX-04 Containing Delta Phase HMX at Elevated Temperatures, *13th APS Topical Conference on Shock Compression of Condensed Matter*, Portland, OR, USA, July 20–25, **2003**, AIP Conference Proceedings 706, p. 1053.

[3] K. S. Vandersall, C. M. Tarver, F. Garcia, P. A. Urtiew, Shock Initiation Experiments on PBX9501 Explosive at 150 °C for Ignition and Growth Modeling, *14th APS Topical Conference on Shock Compression of Condensed Matter*, Baltimore, MD, USA, July 31-August 5, **2005**, AIP Conference Proceedings 845, p. 1127.

[4] F. Garcia, K. S. Vandersall, C. M. Tarver, P. A. Urtiew. Shock Initiation Experiments on the LLM-105 explosive RX-55-AA at 25 °C and 150 °C with Ignition and Growth Modeling, *15th APS Topical Conference on Shock Compression of Condensed Matter*, Kohala Coast, Hawaii, USA, June 24–29, **2007**, AIP Conference Proceedings 955, p. 907.

[5] R. L. Gustavsen, R. J. Gehr, S. M. Bucholtz, R. R. Alcon, B. D. Bartram, Shock initiation of the tri-amino-tri-nitro-benzene based explosive PBX 9502 cooled to −55 °C, *J. Appl. Phys.* **2012**, *112*, 1–16.

[6] R. L. Gustavsen, R. J. Gehr, S. M. Bucholtz, A. H. Pacheco, B. D. Bartram, Shock initiation of the TATB based explosive PBX 9502 heated to 76 °C, *19th Biennial Conference of the APS Topical Group on Shock Compression of Condensed Matter*, Tampa, Florida, USA, June 14–19, **2015**, AIP Conference Proceedings 1793, p, 030017.

[7] R. L. Gustavsen, B. D. Bartram, L. L. Gibson, A. H. Pacheco, J. D. Jones, A. B. Goodbody, Shock initiation of TATB based explosive PBX 9502 heated to 130 °C, *20th Biennial Conference of the APS Topical Group on Shock Compression of Condensed Matter*, St. Louis, Missouri, USA, July 9–14, **2017**, AIP Conference Proceedings 1793, p,100015.

[8] L. Chen, Q. Liu, J. Y. Wu, On shock initiation of heated explosives, *Explosion & Shock Waves* **2013**, *33*, 21–28.

[9] Z. Pi, L. Chen, J. Wu, Temperature-dependent Shock Initiation of CL-20 based High Explosives, *Cent. Eur. J. Energ. Mater.* **2017**, *14*, 361–374.

[10] C. M. Tarver, J. O. Hallquist, L. M. Erickson, Modeling short pulse duration shock initiation of solid explosives, *8th International Symposium on Detonation, Naval Surface Weapons Centre*, Albuquerque, NM, USA, July 15–19, **1985**, p. 951.

[11] J. P. Lu, I. J. Lochert, M. A. Daniel, M. D. Franson, Shock Sensitivity Studies for PBXN-109, *Propellants Explos. Pyrotech.,* **2016**, *41*, 562–571.

[12] H. H. Cady, Coefficient of thermal expansion of pentaerythritoltetranitrate and hexahydro-1,3,5-trinitro-s-triazine(RDX), *J. Chem. Eng. Data*, **1972**, *17*, 369.

[13] R. L. Zuo, J. B. Zhang, J. Zeng, *Metal Materials Science*, Chongqing University Press, Chongqing, **2008**.

[14] K. J. Liao, Y. F. Cong, Y. L. Dai, *Analysis of natural gas and petroleum products*, China Petrochemical Press, Beijing, **2006**.

[15] D. Pirotais, J. P. Plotard, J. C. Braconnier, *Numerical Simulation of Jet Penetration of HMX and TATB Explosives*, 8th Symposium (International) on detonation, Naval Surface Weapons Center, Albuquerque, NM, USA, July 15–19, **1985**, p. 957.

Manuscript received: March 22, 2019
Revised manuscript received: May 18, 2019
Version of record online: July 11, 2019

